Quantitative Measurements of the Size Scaling of Linear and Circular DNA in Nanofluidic Slitlike Confinement

Elizabeth A. Strychalski,*,[†,§] Jon Geist,[‡] Michael Gaitan,[‡] Laurie E. Locascio,[†] and Samuel M. Stavis[‡,§]

[†]Biochemical Science Division, National Institute of Standards and Technology, Gaithersburg, Maryland 20899-1000, United States
[‡]Semiconductor and Dimensional Metrology Division, National Institute of Standards and Technology, Gaithersburg, Maryland 20899-1000, United States

Ⓢ Supporting Information

ABSTRACT: Quantitative size measurements of single linear and circular DNA molecules in nanofluidic slitlike confinement are reported. A novel experimental method using DNA entropophoresis down a nanofluidic staircase implemented comprehensive variation of slitlike confinement around $d \approx 2p$, where d is the slit depth and p is the persistence length, throughout the transition from strong to moderate confinement. A new numerical analysis approximated and corrected systematic imaging errors. Together, these advances enabled the first measurement of an experimental scaling relation between the in-plane radius of gyration, $R_\parallel$, and d, yielding $R_\parallel \sim d^{-1/6}$ for all DNA samples investigated. This differs from the theoretical scaling relation, $R_e \sim d^{-1/4}$, for the root-mean-square end-to-end size, R_e. The use of different labeling ratios also allowed a new test of the influence of fluorescent labels on DNA persistence length. These results improve understanding of the basic physical behavior of polymers confined to nanofluidic slits and inform the design of nanofluidic technology for practical applications.

DNA size decreases as slit depth increases
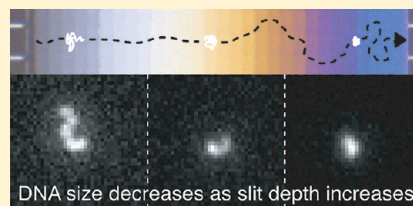
INTRODUCTION

The size of a polymer in solution is one of its most basic physical characteristics. The scaling behavior of polymer size is therefore a central concern in polymer studies and impacts phenomena in other disciplines, such as biophysics, separation science, genetic sequencing, and lab on a chip technology.[1−3] The size of a polymer, such as a DNA molecule, changes upon confinement in nanometer scale fluidic environments. In particular, a polymer in slitlike confinement is squeezed in solution between parallel surfaces forming a shallow slit with depth d. As d is varied, a transition occurs near $d \approx 2p$, where p is the polymer persistence length, between strong[4,5] and moderate[6,7] regimes of slitlike confinement.

Despite considerable effort, and amid continuing investigation, the nature of this transition remains controversial. Over four decades, many theoretical[5,8] and numerical[8−12] studies have been performed of linear polymers in slitlike confinement. More recently, the combination of nanofabricated fluidic devices and fluorescence microscopy has enabled direct measurements of the size of single linear DNA molecules, as characterized by the component of the radius of gyration projected parallel to the slit surfaces, $R_\parallel$, or the in-plane radius of gyration. However, experimental studies have presented conflicting accounts of the variation of $R_\parallel$ with d for linear DNA in nanofluidic slits with $d \approx 2p$.[13−17] Contradictory effects of slitlike confinement have been reported and alternately validated and disputed. In particular, a recent report by Tang et al.[16] disagrees qualitatively with an earlier study by Bonthuis et al.[13] Tang et al. could not reconcile the differences between the two experimental systems and therefore concluded that the cause of this discrepancy remains unclear. This controversy prevents even a qualitative validation of the theoretical scaling

relation, $R_e \sim d^{-1/4}$, for DNA size in strong and moderate confinement as characterized by the root-mean-square end-to-end size, R_e.[5,16] Moreover, none of these experimental studies has reported measured values for a size scaling exponent. In these studies, quantitative measurements of DNA size have been hindered by limited resolution in d, indeterminate or superficial analysis of systematic imaging error, and limitations associated with fluorescence detection, such as measurement errors from photobleaching and uncertainty in labeling ratios and the influence of labels on p. In summary, the effects of slitlike confinement around $d \approx 2p$ on the size of linear polymers, including linear DNA, have eluded both qualitative consensus and quantitative characterization. The size of circular polymers, such as circular DNA, in these systems remains unexplored experimentally.

Two main advances in measurement science are presented here to overcome these limitations and correctly discern the effects of nanofluidic confinement on the size scaling of DNA molecules. First, a novel experimental method using DNA entropophoresis down a nanofluidic staircase achieved comprehensive variation of slitlike confinement throughout the transition from strong to moderate confinement. Second, numerical simulations allowed the most rigorous analysis and correction of systematic imaging error to date. In addition, a judicious selection of experimental conditions eliminated measurement errors due to photobleaching, while the measurement of relative fluorescence labeling ratios allowed a new test of the effects of fluorescence labeling on p. Together, these advances

enabled a quantitative investigation of the size scaling of linear and circular DNA in nanofluidic slitlike confinement around $d \approx 2p$. Experimental size scaling exponents for both polymer morphologies are reported here for the first time. The measurements described here validate measurements by Tang et al.,[16] contradict those of Bonthuis et al.,[13] and give a different experimental size scaling relation than that derived theoretically by Odijk.[16]

The results reported here are of increasing practical importance in nanofluidic technology. For almost two decades, nanofluidic devices incorporating slits have been known to hold great promise for the analysis of long DNA molecules.[18−20] However, many aspects of polymer behavior in these systems remain poorly understood. Quantitative knowledge of the size scaling behavior, in particular, is important for DNA analysis.[2] Nanofluidic devices cannot be designed rationally for this purpose without a clear understanding of the basic physical behavior of polymers confined to nanofluidic slits.

■ EXPERIMENT

A nanofluidic channel with a depth profile approximated by a staircase function with many steps[21] was used to investigate the size of linear and circular DNA by entropophoresis.[22] This directed self-transport resulted in the spontaneous variation of slitlike confinement around $d \approx 2p$, enabling measurements of DNA size with unprecedented resolution in the confining depth. This new method allowed multiplexed measurements of a single DNA molecule variably confined in a single nanofluidic device during a single experiment. This is in contrast to other studies, which required separate nanofluidic devices to vary d. The nanofluidic staircase was fabricated in fused silica and consisted of 30 slitlike steps connected by vertical step edges with depths ranging from approximately 4 to 342 nm and arrayed across a 120 μm wide channel (Figure 1a,b). These depths spanned twice the native DNA persistence length, p, of 51 nm.[3,23] DNA molecules with comparable contour lengths and different morphologies (linear bacteriophage lambda DNA at 48.5 kbp and circular charomid 9−42 DNA at 42.2 kbp) were labeled with the fluorescent dye YOYO-1 at initial ratios of 5 or 20 basepairs per dye molecule for a total of four samples: linear 5:1, linear 20:1, circular 5:1, and circular 20:1. 115, 107, 59, and 129 individual DNA molecules were analyzed for linear 5:1, linear 20:1, circular 5:1, and circular 20:1 samples, respectively. These samples were dispersed in 5X tris borate ethylenediaminetetraacetic acid (TBE) buffer containing 3.0% (volume fraction) 2-mercaptoethanol (Supporting Information). As an initial condition, DNA molecules were driven electrokinetically up the staircase toward shallower steps. The applied electric field was removed. The DNA molecules then spontaneously descended the staircase by entropophoresis and were imaged by widefield epifluorescence microscopy using 40 ms exposures at 5 s intervals (Figure 1c−f).[22] Further details of the device and experiment are described elsewhere.[21,22]

At the onset of entropophoresis, a ratio of summed fluorescence intensities, $I_{5:1}/I_{20:1} \approx 3/2$, was measured for both linear and circular DNA molecules. This differs from $I_{5:1}/I_{20:1} \approx 4$ expected in the case that the 5:1 and 20:1 labeling ratios were achieved. These values show that the intended labeling ratios were not realized in the high ionic strength buffer[24] used here to isolate the steric effects of nanofluidic slitlike confinement (Supporting Information). This suggests the need to validate assumed labeling ratios in related studies. Uncertainty in the labeling ratio is not expected to affect the measurements presented here of the size scaling of DNA molecules (Supporting Information).

DNA size, as characterized by the component of the radius of gyration projected parallel to the $x−y$ plane (Figure 1), $R_{\parallel}$, was extracted from images of single molecules during entropophoresis using custom software. DNA molecules were identified in each image using a region of interest (ROI) of 40 × 40 or 18 × 18 pixels for linear and circular DNA, respectively (Figure 1). Within the ROI, Otsu's method[25] was used to differentiate fluorescence signal from background noise, and connected regions containing ≥8 pixels were identified as comprising the molecule. Fragments and concatemers of
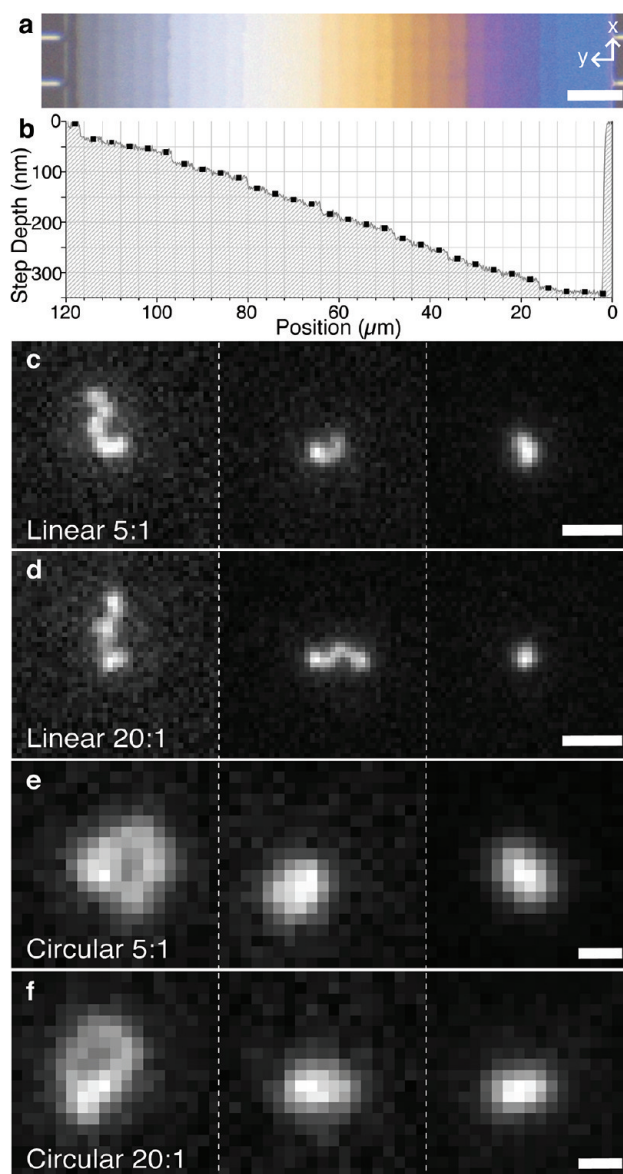

Figure 1. DNA molecules confined to a nanofluidic staircase. A bright-field optical micrograph shows the empty nanofluidic staircase with each step made evident by white light interference (scale bar: 12 μm) (a). Step depths are represented by mean values (black squares), with one standard deviation smaller than the symbols, as well as a scanned probe measurement taken nearest the location in the staircase where DNA molecules were imaged (gray line) (b). Representative fluorescence micrographs of ROIs containing individual linear 5:1 (c), linear 20:1 (d), circular 5:1 (e), and circular 20:1 (f) DNA molecules near the top, middle, and bottom of the staircase, from left to right (scale bar: 3 μm (c, d) and 1 μm (e, f)).

linear DNA were identified by total intensity and area and excluded from further analysis. Assuming homogeneous labeling, the mass of DNA in each pixel was proportional to the pixel intensity, which allowed calculation of the intensity weighted center of mass, $r_{cm}(t)$, and gyration tensor, $G(t)$, for each video frame at time t:

$$r_{cm}(t) = \frac{\sum r(t)I(r, t)}{\sum I(r, t)}$$

$$G(t) = \frac{\sum [r(t) - r_{cm}(t)][r(t) - r_{cm}(t)]I(r, t)}{\sum I(r, t)}$$

where the sum is taken over all pixels comprising the DNA molecule and $I(r,t)$ is the intensity of the pixel at position r. The eigenvalues of this two-dimensional gyration tensor, λ_M and λ_m, with $\lambda_M > \lambda_m$, give the in-plane radius of gyration, $R_\parallel = (\lambda_M + \lambda_m)^{1/2}$.

DNA molecules confined to each step assumed a variety of conformations that can be represented in three dimensions as anisotropic ellipsoids.[10] The approximation of a two-dimensional ellipse has been used widely to characterize $R_\parallel$ for DNA molecules in slitlike confinement.[13,14,16] To interpret DNA molecules as ellipses (Figure 2), the major and minor axes were $4R_M$ and $4R_m$, respectively, where $R_M = (\lambda_M)^{1/2}$ and $R_m = (\lambda_m)^{1/2}$.
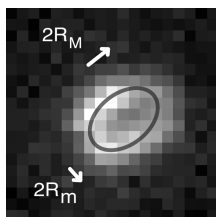

Figure 2. Elliptical interpretation of $R_\parallel$ for a DNA molecule. A fluorescence micrograph shows a circular DNA molecule labeled 20:1 in a 4.6×4.6 μm ROI on a step with a depth of 35 ± 4 nm (mean $\pm$ standard deviation). A representative ellipse, semimajor, $2R_M$, and semiminor, $2R_m$, axes are shown schematically.

Data for unconfined DNA molecules (Supporting Information), once determined to be in focus, were analyzed similarly to data obtained using the staircase. DNA molecules in bulk solution diffused through the depth of field of the microscope objective and were

considered to be in focus when the total area of the DNA molecule was small and approximately constant and $R_\parallel$ continued to fluctuate. Out of focus DNA molecules were characterized by significantly larger areas and lower signal-to-noise ratios.

For each step of the staircase and for bulk solution, R_M and R_m values were placed into 10 nm histogram bins, which were normalized and fit to probability distributions for either DNA molecules in slitlike confinement[13]

$$P_{\text{slit}}(R) = \exp[-R^2/\sigma] \exp[-R_{\text{mod}}(R_{\text{mod}} - R_{\text{min}})^3 \\ /(\sigma(R - R_{\text{min}})^2)] \tag{1}$$

or for unconfined DNA molecules in bulk solution[7]

$$P_{\text{bulk}}(R) = \exp[-R^2/\sigma] \exp[-2R_{\text{mod}}(R_{\text{mod}} - R_{\text{min}})^4 \\ /(3\sigma(R - R_{\text{min}})^3)]$$

where R represents R_M or R_m, the first exponential describes extended conformations, the second exponential describes compact conformations, σ depends on the physical attributes of the DNA molecule, R_{mod} gives the mode of the size distribution, and R_{min} is the smallest value of R (Figure 3). A nonlinear least-squares fitting algorithm provided statistical uncertainties for the parameters σ, R_{min}, and R_{mod}.

Although eq 1 was derived by Flory for the radius of gyration of a flexible linear polymer in two dimensions,[7] these probability distributions were used here for measurements of $R_\parallel$ for semiflexible, linear, and circular DNA molecules and slit depths that spanned the transition between two and three dimensions. On the shallowest steps of the staircase, extended conformations of circular DNA molecules were depopulated relative to linear DNA molecules (Figure 3c,d). This
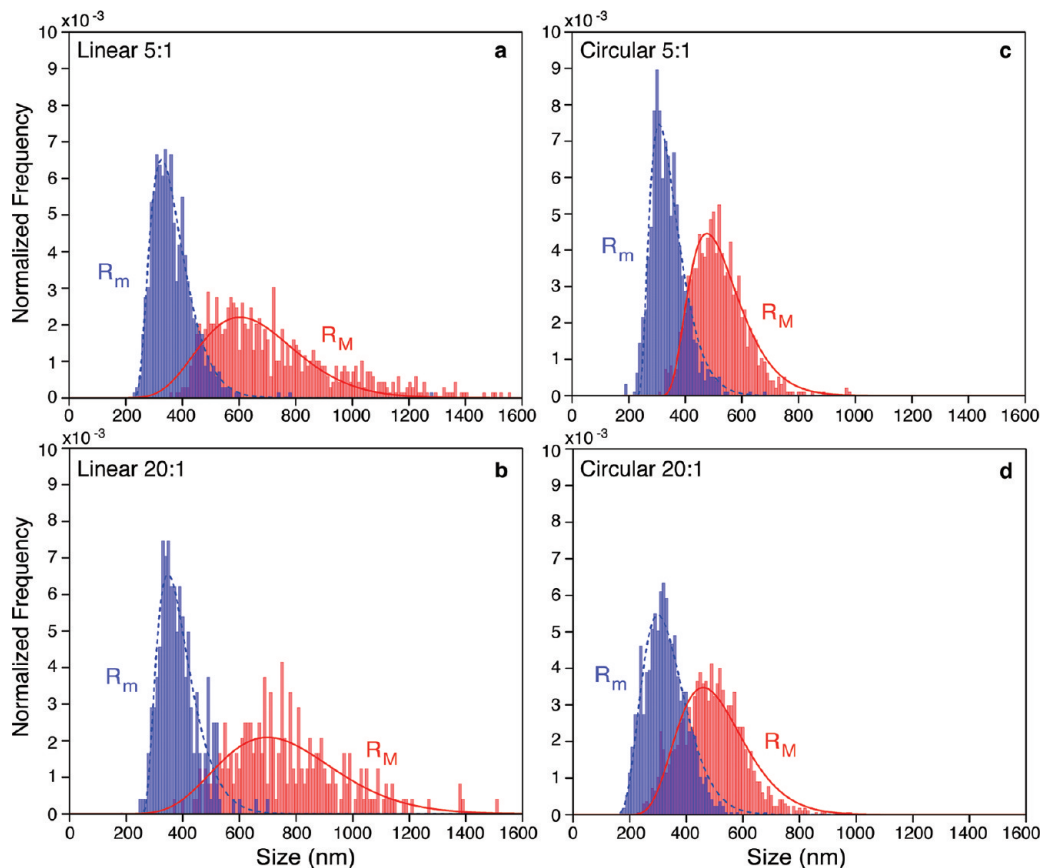

Figure 3. Size distribution measurements. Representative normalized histograms and probability distribution fits used to determine mode values for R_M (red, solid line) and R_m (blue, dash line) are shown for linear 5:1 (a), linear 20:1 (b), circular 5:1 (c), and circular 20:1 (d) DNA samples for a step depth of 35 ± 4 nm (mean $\pm$ standard deviation). A few instances of R_M values of nearly 2.3 and 1.8 μm were observed for (a) and (b), respectively, but are not plotted here.
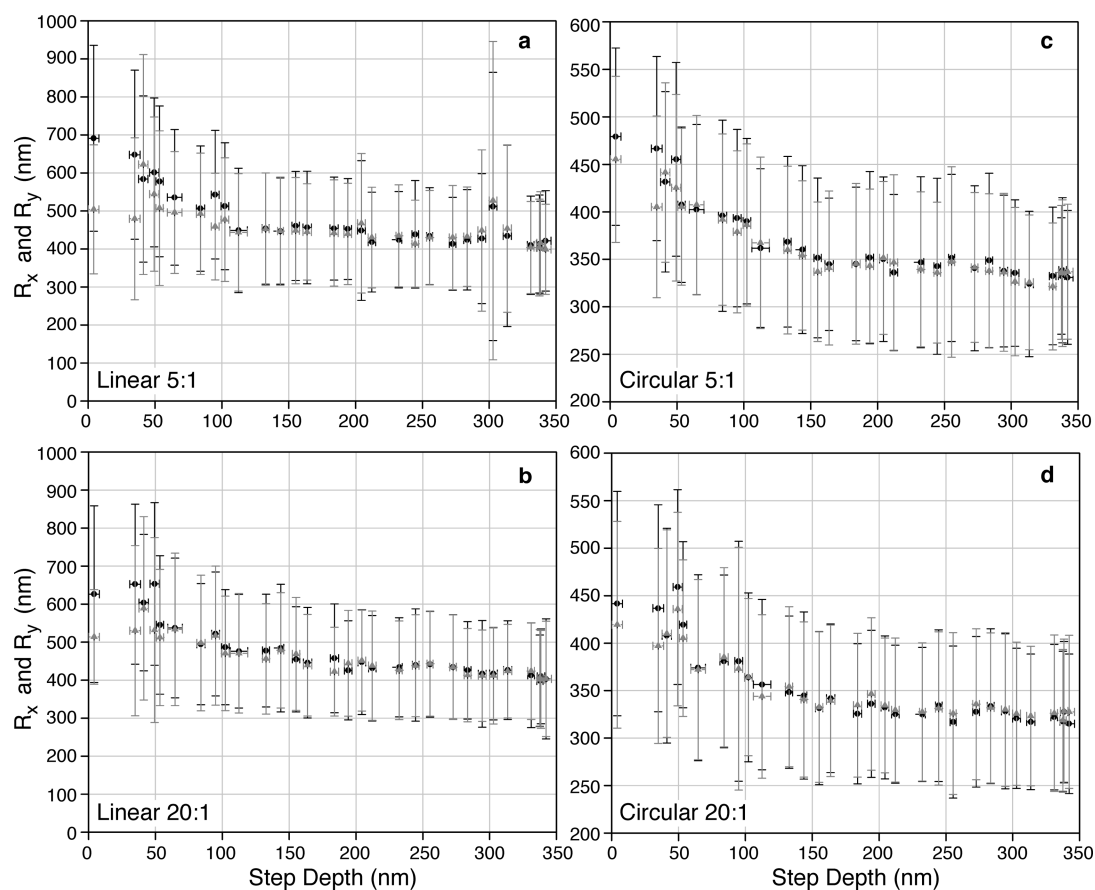
Figure 4. Orientation of DNA molecules during entropophoresis. Components of $R_\parallel$ along the x-axis of the staircase, R_x (black circles), and along the y-axis of the staircase, R_y (gray triangles), as a function of step depth are shown for linear 5:1 (a), linear 20:1 (b), circular 5:1 (c), and circular 20:1 (d) DNA samples. Data points are mean values. X-axis bars represent one standard deviation. Y-axis bars represent one standard deviation and contain contributions from measurement error but are dominated by the physical fluctuation of the size of the DNA molecules. DNA molecules exhibited some tendency to orient across the staircase on the shallowest steps, especially for the linear morphology. This may be due in part to electrostatic effects at step edges or relatively long rotational relaxation times for DNA molecules in these very shallow slits.[16] In general, however, molecules entropophoresed down the staircase without a preferred orientation induced by interactions with step edges.

suggests the need for the future development of a probability distribution that more accurately models the effect of a circular morphology on the size of semiflexible polymers in slitlike confinement through this transition. For all DNA size distributions, similar trends in size variation were obtained and similar conclusions were drawn using either the fitted mode or the mean values of $R_\parallel$.

During entropophoresis, DNA molecules spanned, at most, one step edge at a time, and the variation of slitlike confinement was sufficiently slow[22] to allow the DNA molecules to relax between interactions with the step edges. Components of $R_\parallel$ along the x- and y-axes of the staircase showed no significant average orientation during transport (Figure 4), which would have indicated departure from equilibrium as preferential extension along a particular direction. In a test to determine whether interactions with step edges affected measured $R_\parallel$ values, images with the molecular center of mass within 1.0, 0.5, or 0 μm of either side of each step edge were selectively excluded from analysis. In all cases, mode values of fits to the frequency histogram for $R_\parallel$ were in good agreement. The mode was also insensitive to the relatively small number of perturbed conformations induced by interactions with step edges (Figure 5). For these reasons, and to maximize single molecule statistics, all data were included for the results presented here.

Systematic imaging errors from optical diffraction and camera pixelation of fluorescent DNA molecules in solution are intrinsic both to the measurements reported here and previous related experimental studies. These imaging errors were approximated and corrected here as an integral component of quantitative measurements of $R_\parallel$ (Figure 6).

Each DNA molecule remained in focus during entropophoresis down the staircase because all steps were within the depth of field of the microscope objective lens. However, the true conformations were not accessible optically, as DNA molecules fluctuated during each camera exposure, and different portions of the contour length may have been in proximity or overlapped at a length scale below the optical diffraction limit and camera pixel size. As an approximation, the most probable in-plane shapes of the DNA molecules were modeled as ellipses of uniform fluorescence intensity with a range of R_M and R_m values encompassing the measured experimental values. This enabled measurements to be related with high precision to corresponding elliptical models. A library was populated with major and minor axis values, incremented by 51 and 54 nm, respectively, which produced model ellipses of varied size and anisotropy. Imaging by wide-field epifluorescence microscopy was then simulated in two steps, as shown in Figure 6a−c. First, model ellipses representing DNA molecules were blurred with a two-dimensional Gaussian filter, which has been shown to be an accurate approximation of the Airy function for a nonparaxial wide-field fluorescence microscope.[26,27] Using the known optical properties of the fluorescent DNA molecules, the nanofluidic device, and the microscope system (Supporting Information Table 1), the standard deviation of this Gaussian distribution and the Airy radius were calculated to be 80.6 and 227 nm, respectively. These calculations were favored over an experimental determination of the point spread function, because the accuracy of such a measurement may be compromised by difficulty in obtaining a point source with an emission spectrum identical to that of YOYO-1 bis-intercalated into double-stranded DNA, as well as by large errors that may occur when a
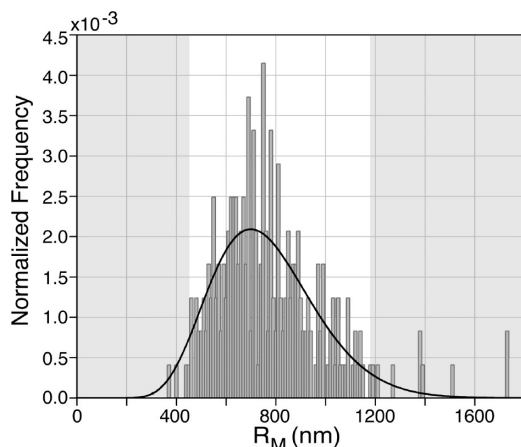
Figure 5. Robustness of fitted mode values. This plot of R_M values for linear DNA molecules labeled 20:1 on a step with a depth of 35 ± 4 nm (mean ± standard deviation) is representative of the poorest quality data analyzed in this way. These data are expected to most clearly manifest difficulties in obtaining reliable mode values, as well as the advantage of reporting mode, rather than mean, values with these small data sets. The linear morphology has the potential to become more elongated and perturbed from equilibrium than the circular morphology by interactions with step edges, which would have been most pronounced between the shallowest steps and would have shifted values of R_M and R_m in opposite directions away from the mode value. For example, a very elongated molecule transiting a step edge is represented in the data as a relatively very large R_M value and a corresponding very small R_m value. The exclusion of data in either of the gray regions from the fit to determine the mode value alters that value by <0.3%, indicating that the mode value is decidedly insensitive to data in the tails of this fitted distribution. This result underscores the robustness of the mode determination for data sets that may contain spurious data with extremely small or large values.

two-dimensional Gaussian distribution is fit to an image of a point source with a pixel size exceeding the standard deviation of the Gaussian distribution.[26] The Gaussian filter was truncated at the Airy radius and applied to the model elliptical DNA molecules. Next, the blurred model objects were binned into pixel elements of 254 × 254 nm, as obtained from the objective magnification of 63× and the camera pixel size of 16 × 16 μm. While a higher magnification objective would have resulted in a smaller effective pixel size and reduced corrections due to pixelation error, the larger field of view provided by the objective used here was necessary to image DNA molecules descending the entire 120 μm width of the staircase. The ratios of R_M and R_m values for corresponding model ellipses and simulated images provided corrections to the experimental data as a function of experimental R_M and R_m values.

As the major and minor axes of the model ellipse were incrementally increased, the corresponding imaging correction showed a rippling phenomenon with periodic peaks and troughs (Figure 6d). This rippling resulted from the fixed relationship between the model ellipses and simulated camera pixel array. To account for the random location and orientation of experimentally measured DNA molecules relative to the actual camera pixel array, this rippled imaging correction was smoothed by a polynomial fitting function. This function consisted of third-order polynomials for the major and minor axes and a first-order cross-term, which approximated the low order curvature of the imaging correction and neglected the higher order rippling effect. Thus, a smoothed imaging correction function was defined and applied to the experimental mode values of R_M and R_m for each step (Figure 6e).

In this way, systematic imaging errors were estimated to have resulted in measured values of $R_\parallel$ that exceeded the actual values by 1−7% for the experimental system used here. The corresponding imaging corrections became more significant as $R_\parallel$ values decreased, with measured bulk solution values of $R_\parallel$ decreased by the most significant correction. This analysis has several implications. The measured $R_\parallel$ value for a given d was reasonably robust against diffraction-limited
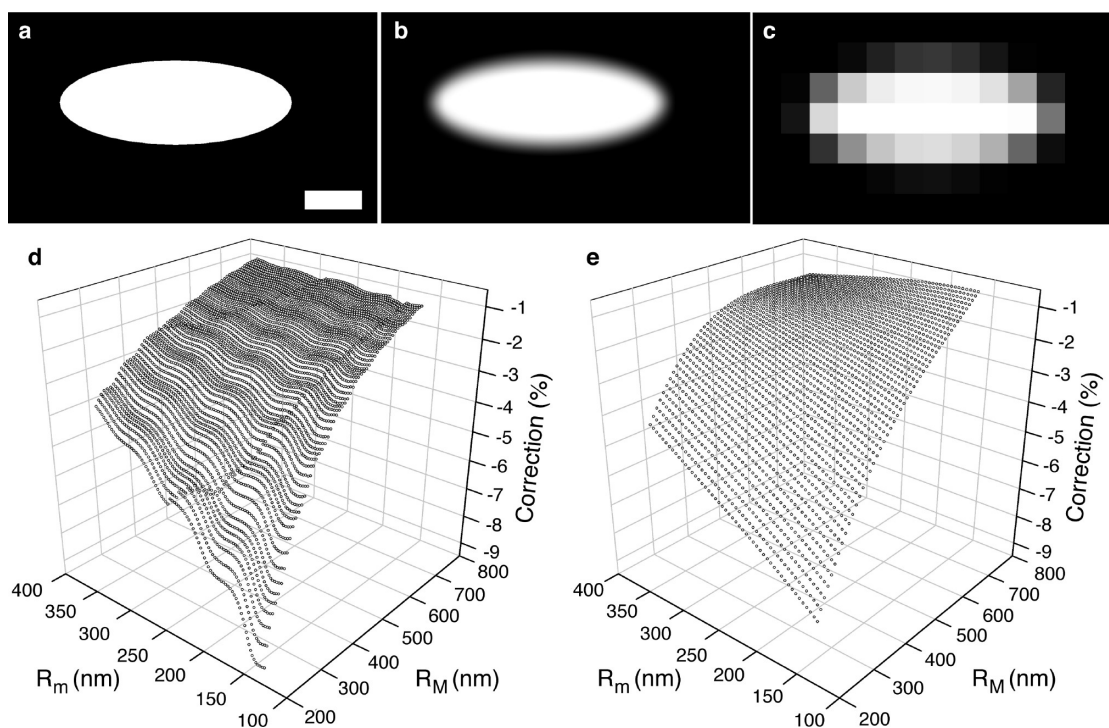

Figure 6. Systematic imaging error correction. The effects of optical diffraction and camera pixelation on measured values of $R_\parallel$ were approximated, simulated, and corrected. A model ellipse (a), the ellipse blurred according to the optical point spread function (b), and the ellipse blurred and pixelated according to the finite camera pixel size (c) representing a DNA molecule are shown. These transformations enlarged the apparent size of the molecule (scale bar: 700 nm). The correction between $R_\parallel$ values calculated for the original model ellipses (as in (a)) and the experimentally accessible blurred and pixelated ellipses (as in (c)) are plotted versus the experimentally accessible R_M and R_m values (d). The data in (d) were fit to provide the final correction (e).
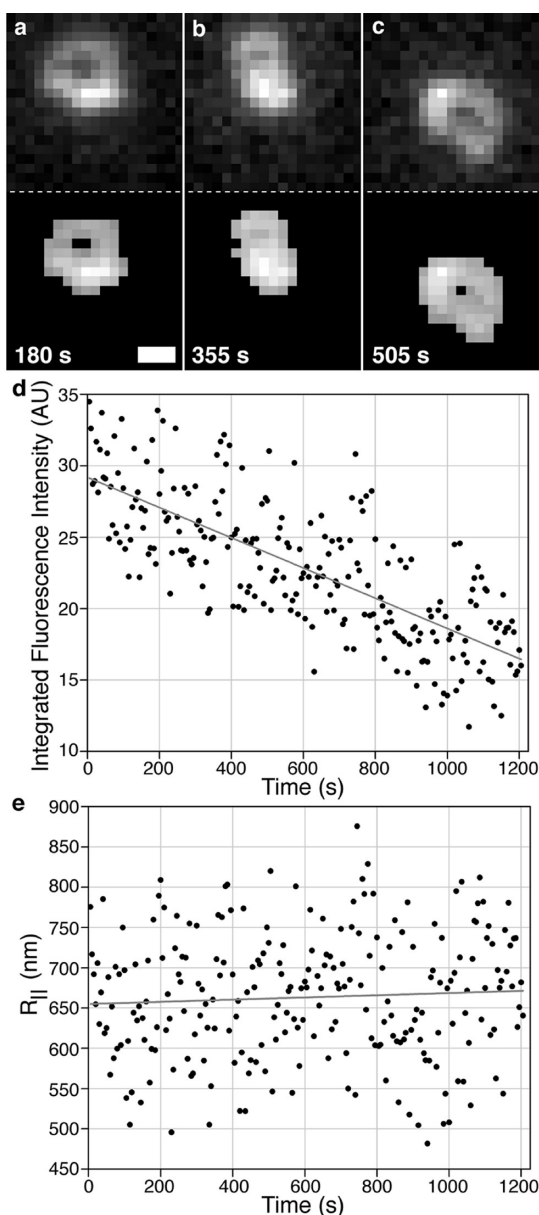
Figure 7. Effect of photobleaching on $R_{\parallel}$ values. The size of a circular DNA molecule labeled 5:1 fluctuated on the shallowest step with a depth of 4 ± 4 nm (mean $\pm$ standard deviation) (a–c) (scale bar: 1 μm). The upper images are unprocessed fluorescence micrographs of ROIs containing a single DNA molecule, which are shown in the lower images after analysis to identify pixels comprising the molecule. The total fluorescence intensity of the molecule decreased during observation (d). However, this decrease in intensity had no significant effect on measured $R_{\parallel}$ values (e). These data have been corrected for the diffraction-limited blurring and camera pixelation similarly to the mode values. The scatter in (e) resulted from the natural Brownian fluctuation of the molecule. Gray lines in (d) and (e) represent linear fits to the data, giving slopes of -0.0106 ± 0.0006 and 0.014 ± 0.015 (mean $\pm$ standard deviation), respectively. Each data symbol corresponds to a value obtained from a single image.

blurring and camera pixelation. However, because the systematic imaging errors varied with d, corrections for these errors had an important aggregate effect on the size scaling analysis, as described below. In contrast, normalization by the bulk solution $R_{\parallel}$ value, and the associated imaging correction, did not influence analysis of scaling exponents due to the constant effect of normalization. This analysis supersedes a simpler correction[28] and is the most rigorous treatment

to date of systematic imaging errors of DNA molecules in nanofluidic slitlike confinement.

Photobleaching is also a significant concern in single molecule fluorescence analysis.[16] However, the size measurements performed here were determined to be robust against reduction in the signal-to-noise ratio from this effect (Figure 7). Several DNA molecules paused for extended periods of time, but were not adsorbed irreversibly, on a single step near the top of the staircase. This rare behavior may have resulted from electrostatic or steric interactions that occurred between these molecules and the surfaces of the staircase structure. These immobilized DNA molecules were excluded from the analysis of size scaling but facilitated a test of the effects of dye photobleaching on the measured $R_{\parallel}$ values. During observation, the center of mass of these DNA molecules did not descend the staircase, but the molecular conformations continued to fluctuate due to Brownian motion. Photobleaching resulted in decreased integrated fluorescence intensities of these DNA molecules but did not bias $R_{\parallel}$ values. These results demonstrate that the signal-to-noise ratio of single molecule detection remained sufficiently high throughout the experiment for a robust analysis of single DNA molecules using the methods employed here.

■ RESULTS AND DISCUSSION

Together, the nanofluidic staircase and systematic imaging error corrections enabled quantitative measurements of $R_{\parallel}$ for DNA molecules throughout the transition between strong and moderate regimes of slitlike confinement. Corrected $R_{\parallel}$ values are presented normalized by corresponding measured bulk solution values (Figure 8), without normalization (Supporting Information Figure 1), and without correction or normalization (Supporting Information Figure 2). $R_{\parallel}$ data for the shallowest step are shown for completeness but were excluded from further analysis, due to the relatively large surface roughness compared to d for this step.[21]

Measured sizes for all DNA samples generally decreased as d increased from strong confinement, through $d \approx 2p$, to moderate confinement. The trends in size variation observed here validate measurements reported by Tang et al.[16] and contradict those of Bonthuis et al.[13] (Figure 9 and Table 1). The previous results of Strychalski et al.[15] also do not follow the trend reported by Bonthuis et al.[13] but cannot be compared directly here, due to limited confinement resolution and lack of DNA size measurements in bulk solution for normalization. Bonthuis et al.[13] reported the abrupt onset of a saturation regime in DNA size for strong confinement near $d \approx 2p$, which was not observed here or by Tang et al.[16] In contrast to Bonthuis et al.,[13] Tang et al.[16] measured a monotonic decrease in DNA size with decreasing confinement that suggested a gradual transition between confinement regimes. Tang et al.[16] did not develop a quantitative experimental scaling relation, due to known biases from optical diffraction and photobleaching, but revisited the most recent theoretical derivation by Odijk[5] of the scaling relation $R_e \sim d^{-1/4}$. This scaling relation, which has not been verified experimentally, provides the most relevant theoretical framework to analyze the experimental results reported here.

To establish an experimental scaling relation between $R_{\parallel}$ and d and compare this to the theoretical relation, a power law function was fit to the data presented here (Figure 8, Figure 10, and Table 2). Size scaling exponents obtained from separate fits to the uncorrected and corrected data differ significantly, emphasizing the importance of correcting for systematic imaging errors. Based on the goodness of fit parameters for fits to the corrected data (Table 2), a single power law models the system reasonably well. The size scaling relation of $R_{\parallel} \sim d^{-1/6}$ obtained from the corrected data is in excellent agreement with
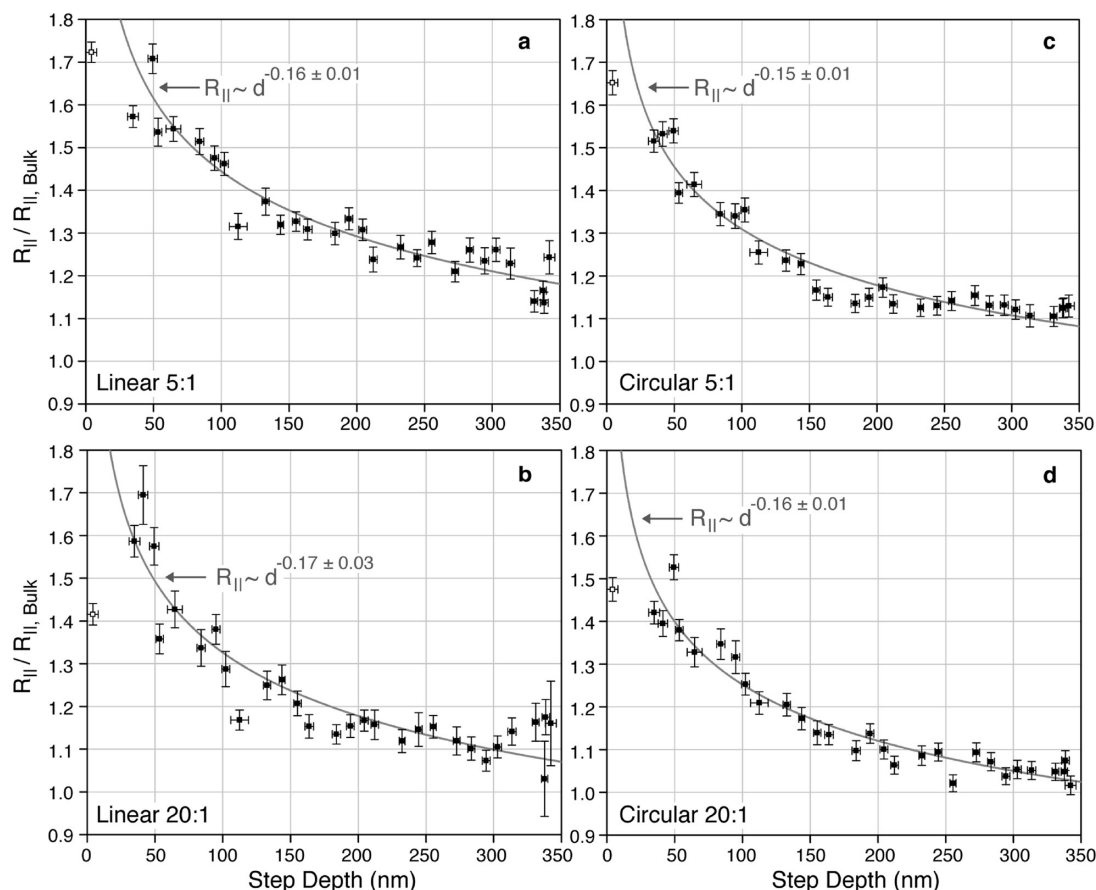
Figure 8. Size measurements. Fitted mode values of $R_{\parallel}$ were corrected for systematic imaging error and normalized by the corresponding corrected bulk solution $R_{\parallel}$ values, $R_{\parallel,Bulk}$, for linear 5:1 (a), linear 20:1 (b), circular 5:1 (c), and circular 20:1 (d) DNA samples. DNA size generally decreased with increasing step depth, d. Power law fits (gray line) yielded size scaling exponents reported as mean $\pm$ standard deviation. Corrected bulk solution values of $R_{\parallel}$ were 430 $\pm$ 5 nm (linear 5:1), 485 $\pm$ 7 nm (linear 20:1), 366 $\pm$ 6 nm (circular 5:1), and 377 $\pm$ 6 nm (circular 20:1) (mean $\pm$ standard deviation). X-axis bars represent one standard deviation. Y-axis bars represent one standard deviation of the fitted mode value and one standard deviation of the fitted bulk mode value added in quadrature and do not account for other sources of error. Data for the shallowest step (open square) were excluded from analysis.

a fit also performed here to the uncorrected data of Tang et al.[16] for $d \approx 32-565$ nm (not shown) that gave an exponent of -0.17 ± 0.01 (mean $\pm$ standard deviation). The microscope system used by Tang et al.[16] had a higher magnification objective lens with an identical numerical aperture and smaller pixel size compared to the microscope system used here. This would have reduced pixelation error but would not have reduced error from optical diffraction compared to the measurements made here. Further quantitative comparison between the corrected data reported here and the uncorrected data of Tang et al.[16] would require a full characterization of systematic errors, including photobleaching. However, in all cases, the experimental size scaling exponents fitted here to measurements of $R_{\parallel}$ differ significantly from the theoretical value predicted for the variation of R_e with d.

The two fluorescent labeling ratios used here also enabled a new test of the equilibrium effects of YOYO-1 on p. First, consider the two linear DNA samples. The measured ratio of summed fluorescence intensities, $I_{5:1}/I_{20:1} \approx 3/2$, resulted from different numbers of dye molecules per DNA molecule. It is known that the bis-intercalation of YOYO-1 dye molecules into a DNA molecule extends its contour length, L,[3] giving different values of L for the two linear DNA samples. Despite these different L values, linear 5:1 and linear 20:1 DNA samples had nearly identical corrected $R_{\parallel}$ values without normalization for

all d (Supporting Information Figure 3). This was also measured for circular 5:1 and circular 20:1 DNA samples. Then, consider Odijk's scaling relation $R_e \sim L^{3/4}p^{1/4}w^{1/4}d^{-1/4}$, which applies throughout $d \approx 2p$ for linear DNA.[5] If this relation holds for $R_{\parallel}$, and assuming equal scaling coefficients and effective widths, w, for the two linear DNA samples, then p decreased as labeling increased. This prediction agrees qualitatively with a nonequilibrium study of the same effect.[29] The present analysis must be viewed as approximate, however, as the size scaling exponents reported here do not validate this theoretical scaling relation. Moreover, w may vary with labeling ratio.[30] Additional study is required to understand this important effect.

■ CONCLUSION

Size scaling exponents were measured for the first time for linear and circular DNA in nanofluidic slitlike confinement around $d \approx 2p$. Size measurements of linear DNA qualitatively and semiquantitatively validate those of Tang et al.[16] and qualitatively contradict those of Bonthuis et al.[13] Specifically, power law fits to measurements of the DNA samples investigated here and the data reported by Tang et al.[16] gave size scaling relations of $R_{\parallel} \sim d^{-1/6}$ throughout the $d \approx 2p$ transition. This experimental scaling relation differs from the

Table 1. Comparison of Experimental Systems for Size Measurements of Linear DNA through the Transition from Strong to Moderate Slitlike Confinement

| report	DNA sample	buffer system	fluorescent label	experimental temperature	buffer viscosity	surface roughness
this report	Lambda Phage, 48.5 kbp	5X TBE (650 mM tris base, 225 mM boric acid, 12.5 mM ethylenediaminetetraacetic acid), 3% (volume fraction) β-mercaptoethanol	YOYO-1, prepared at 5:1 bp:dye, measured as lower	27.0 ± 0.1 °C (mean ± limit of error)[22]	1.254 × 10^{-3} ± 0.004 × 10^{-3}) Pa·s at 27.0 °C (mean ± std dev)[22]	etched surface: 2.9 ± 0.3 nm (mean ± std dev); cover surface: <0.5 nm[21]
Tang et al.[16]	Lambda Phage, 48.5 kbp	1.5X TBE (270 mM tris base, 270 mM boric acid, 6 mM ethylenediaminetetraacetic acid), 4% (volume fraction) β-mercaptoethanol, 12.5 mg/mL glucose, 0.16 mg/mL glucose oxidase, 9.6 μg/mL catalase	YOYO-1, prepared at 4:1 bp:dye, not measured	not reported	1.17 × 10^{-3} Pa·s at 22.5 °C	not reported
Bonthuis et al.[13]	Lambda Phage, 48.5 kbp	50 mM NaCl, 10 mM tris-ethylenediaminetetraacetic acid, 0.07% (volume fraction) dimethyl sulfoxide	YOYO-1, prepared at 6:1 bp:dye, not measured	not reported	not reported	not reported
Strychalski et al.[15]	Lambda Phage, 48.5 kbp	5X TBE, 2% (volume fraction) volume fraction β-mercaptoethanol	YOYO-1, prepared at 5:1 bp:dye, not measured	not reported	not reported	<1.2 nm (rms)
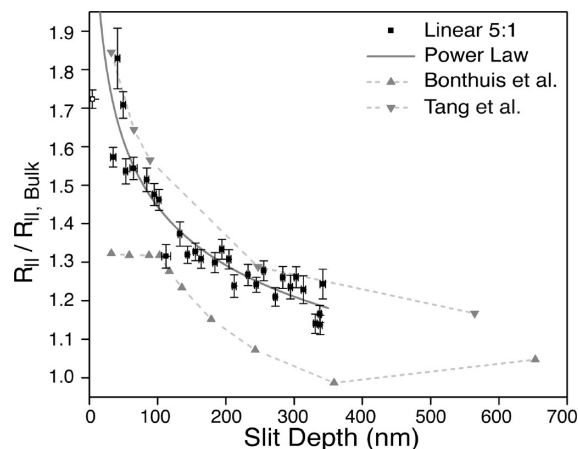
Figure 9. Interstudy comparison. Contending measurements of the size variation of lambda phage DNA molecules in nanofluidic slitlike confinement are shown, and the experimental systems are compared in Table 1. Of the four samples studied here, linear DNA labeled 5:1, corrected for systematic imaging errors and normalized by the corresponding measured bulk solution value, was selected as most directly comparable to Bonthuis et al.[13] and Tang et al.[16] Data from these studies were obtained manually from plots as published. The trend in size variation measured here contradicts that reported by Bothuis et al.[13] and validates that reported by Tang et al.[16] This interstudy comparison emphasizes the confinement resolution and quantitative measurements of the size scaling exponent achieved here.

Table 2. Comparison of Size Scaling Exponents for Fits to Corrected and Uncorrected Experimental Data[a]

DNA sample	scaling exponent for corrected data	adjusted R^2	reduced χ^2	scaling exponent for uncorrected data
linear 5:1	−0.16 ± 0.01	0.88	0.003	−0.10 ± 0.01
linear 20:1	−0.17 ± 0.03	0.86	0.004	−0.09 ± 0.01
circular 5:1	−0.15 ± 0.01	0.93	0.001	−0.10 ± 0.01
circular 20:1	−0.16 ± 0.01	0.92	0.002	−0.09 ± 0.01

[a]Adjusted R^2 and reduced χ^2 are given for fits to the corrected data. Scaling exponents resulted from unweighted, nonlinear least-squares fitting algorithms and are reported as mean ± standard deviation. A single power law is a reasonable model for the system, as indicated by the goodness of fit parameters. However, fitted scaling exponents differ from the hypothetical scaling relation $R_{\parallel} \sim d^{-1/4}$ in all cases.

theoretical scaling relation, $R_e \sim d^{-1/4}$, derived by Odijk.[5] The size measurements reported here also suggest a decreased persistence length as the fluorescence labeling ratio increased. These results clarify topics of enduring interest in polymer physics and increasing importance for practical applications of nanofluidic technology.

The advances reported here also highlight the need for future work in several areas. First, while a uniform ellipse is a reasonable approximation of the two-dimensional projection of the most probable shape for an ensemble of images of DNA molecules, this simple model is less accurate for an image of a single DNA molecule. Realistic numerical simulations of DNA conformations in varied slitlike confinement are needed to provide single molecule object and image distributions and give an exact imaging correction. Second, the discrepancy between the theoretical scaling relations for $R_e \sim d^{-1/4}$ and $R_{\parallel} \sim d^{-1/6}$ could be clarified experimentally by tracking the relative positions of end labels bound to DNA molecules to measure R_e,
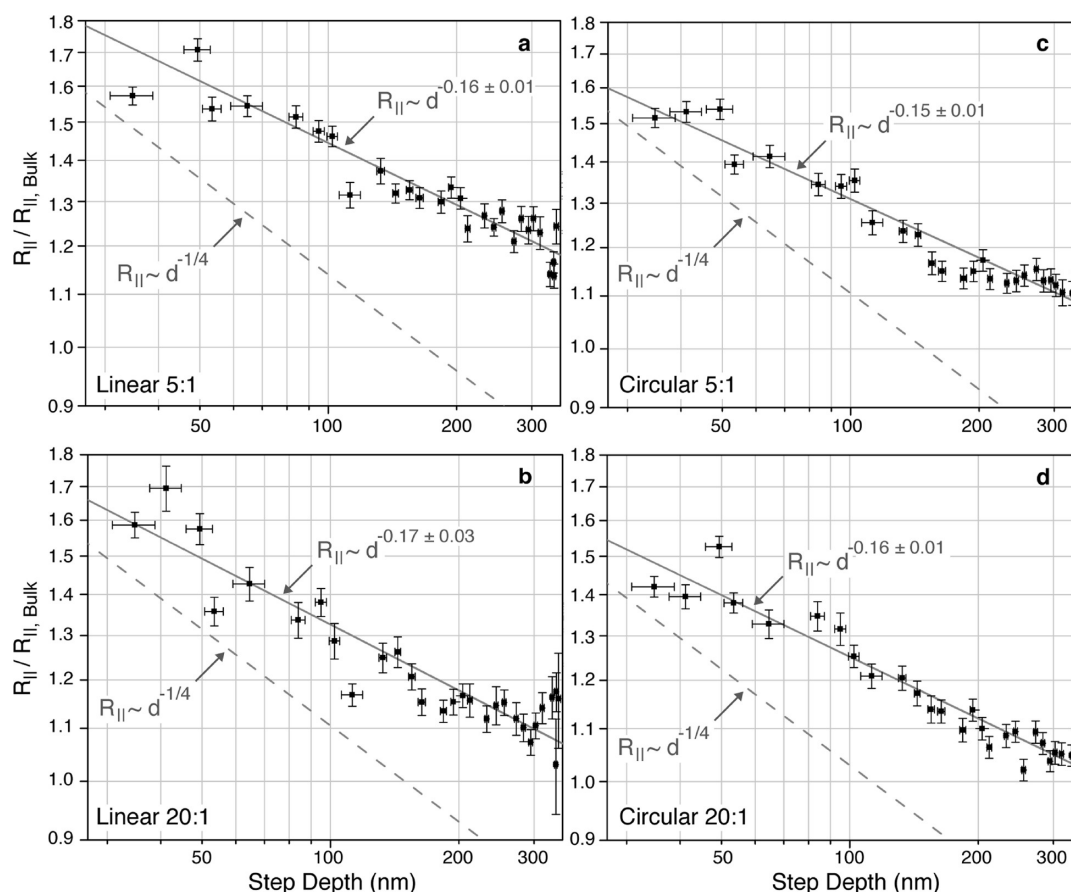
Figure 10. Corrected $R_{\parallel}$ values normalized by bulk solution values and plotted using log–log axes. Fitted mode values of $R_{\parallel}$ as a function of step depth, d, are shown for linear 5:1 (a), linear 20:1 (b), circular 5:1 (c), and circular 20:1 (d) DNA samples. The x-axis and y-axis bars represent one standard deviation. These data have been corrected for systematic optical imaging errors and normalized by corresponding corrected bulk solution values. A hypothetical scaling relation $R_{\parallel} \sim d^{-1/4}$ (offset dashed gray lines) differs from power law fits (solid gray lines) to the experimental data. Fitted exponents are reported as mean $\pm$ standard deviation.

theoretically by deriving a scaling relation for $R_{\parallel}$, or numerically by establishing a relation between R_e and $R_{\parallel}$. Third, a more sophisticated statistical analysis is needed to determine how accurately a single power law model describes the system and the extent to which morphology affects DNA size in slitlike confinement around $d \approx 2p$. Finally, progress is needed in measuring absolute numbers of dye molecules labeling individual DNA molecules and understanding the effects of fluorescence labeling on p.

■ ASSOCIATED CONTENT

Ⓢ Supporting Information

Further discussion describes the buffer solution, influence of the fluorescence labeling ratio on measurements of the size scaling exponent, size measurements in bulk solution, and optical properties of the experimental system. Additional figures show corrected size measurements without normalization, size measurements without correction or normalization, and a direct comparison of measured corrected sizes without normalization. This material is available free of charge via the Internet at http://pubs.acs.org.

■ AUTHOR INFORMATION

Corresponding Author
*E-mail: elizabeth.strychalski@nist.gov.

Author Contributions
§These authors contributed equally.

■ REFERENCES

(1) Levy, S. L.; Craighead, H. G. *Chem. Soc. Rev.* **2010**, *39*, 1133–1152.
(2) Salieb-Beugelaar, G. B.; Dorfman, K. D.; van den Berg, A.; Eijkel, J. C. T. *Lab Chip* **2009**, *9*, 2508–2523.
(3) Persson, F.; Tegenfeldt, J. O. *Chem. Soc. Rev.* **2010**, *39*, 985–999.

(4) Odijk, T. *Macromolecules* **1983**, *16*, 1340−1344.

(5) Odijk, T. *Phys. Rev. E* **2008**, *77*, 060901.

(6) Daoud, M.; de Gennes, P. G. *J. Phys. (Paris)* **1977**, *38*, 85−93.

(7) de Gennes, P.-G. *Scaling Concepts in Polymer Physics*; Cornell University Press: Ithaca, NY, 1985.

(8) Chaudhuri, D.; Mulder, B. *Phys. Rev. E* **2011**, *83*, 031803.

(9) Van Vliet, J. H.; Luyten, M. C.; ten Brinke, G. *Macromolecules* **1992**, *25*, 3802−3806.

(10) Van Vliet, J. H.; Luyten, M. C.; ten Brinke, G. *J. Chem. Phys.* **1990**, *93*, 1436−1441.

(11) Wall, F. T.; Mandel, F.; Chin, J. C. *J. Chem. Phys.* **1976**, *65*, 2231−2234.

(12) Jeon, J.; Chun, M.-S. *J. Chem. Phys.* **2007**, *126*, 154904.

(13) Bonthuis, D. J.; Meyer, C.; Stein, D.; Dekker, C. *Phys. Rev. Lett.* **2008**, *101*, 108303.

(14) Lin, P. K.; Fu, C. C.; Chen, Y. L.; Chen, Y. R.; Wei, P. K.; Kuan, C. H.; Fann, W. S. *Phys. Rev. E* **2007**, *76*, 011806.

(15) Strychalski, E. A.; Stavis, S. M.; Craighead, H. G. *Nanotechnology* **2008**, *19*, 315301.

(16) Tang, J.; Levy, S. L.; Trahan, D. W.; Jones, J. J.; Craighead, H. G.; Doyle, P. S. *Macromolecules* **2010**, *43*, 7368−7377.

(17) Uemura, H.; Ichikawa, M.; Kimura, Y. *Phys. Rev. E* **2010**, *81*, 051801.

(18) Volkmuth, W. D.; Austin, R. H. *Nature* **1992**, *358*, 600−602.

(19) Han, J.; Craighead, H. G. *Science* **2000**, *288*, 1026−1029.

(20) Cross, J. D.; Strychalski, E. A.; Craighead, H. G. *J. Appl. Phys.* **2007**, *102*, 024701.

(21) Stavis, S. M.; Strychalski, E. A.; Gaitan, M. *Nanotechnology* **2009**, *20*, 165302.

(22) Stavis, S. M.; Geist, J.; Gaitan, M.; Locascio, L. E.; Strychalski, E. A. *Lab Chip* **2012**, DOI: 10.1039/C2LC21152A.

(23) Bouchiat, C.; Wang, M. D.; Allemand, J. F.; Strick, T.; Block, S. M.; Croquette, V. *Biophys. J.* **1999**, *76*, 409−413.

(24) Gunther, K.; Mertig, M.; Seidel, R. *Nucleic Acids Res.* **2010**, *38*, 6526−6532.

(25) Otsu, N. *IEEE Trans. Syst. Man Cybern.* **1979**, *9*, 62−66.

(26) Thompson, R. E.; Larson, D. R.; Webb, W. W. *Biophys. J.* **2002**, *82*, 2775−2783.

(27) Zhang, B.; Zerubia, J.; Olivo-Marin, J. C. *Appl. Opt.* **2007**, *46*, 1819−1829.

(28) Strychalski, E. A.; Levy, S. L.; Craighead, H. G. *Macromolecules* **2008**, *41*, 7716−7721.

(29) Murade, C. U.; Subramaniam, V.; Otto, C.; Bennink, M. L. *Biophys. J.* **2009**, *97*, 835−843.

(30) Reisner, W.; Beech, J. P.; Larsen, N. B.; Flyvbjerg, H.; Kristensen, A.; Tegenfeldt, J. O. *Phys. Rev. Lett.* **2007**, *99*, 058302.